

Projections  
Algebraic methods  
Back projection  
Filtered back projections  
Fourier transform techniques  
Estimation of resolution

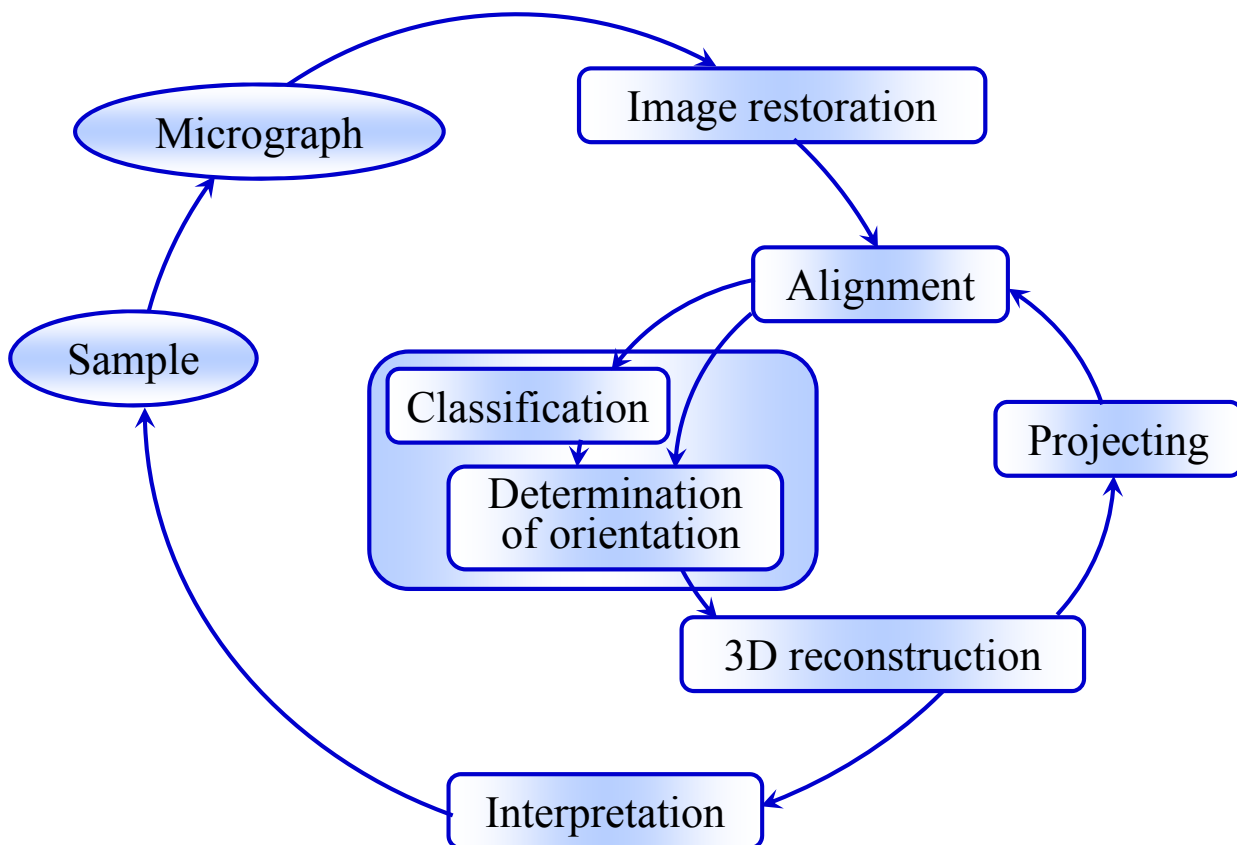
Cryo EM & 3D Image Processing  
6 July 2016  
Thiruvananthapuram, India



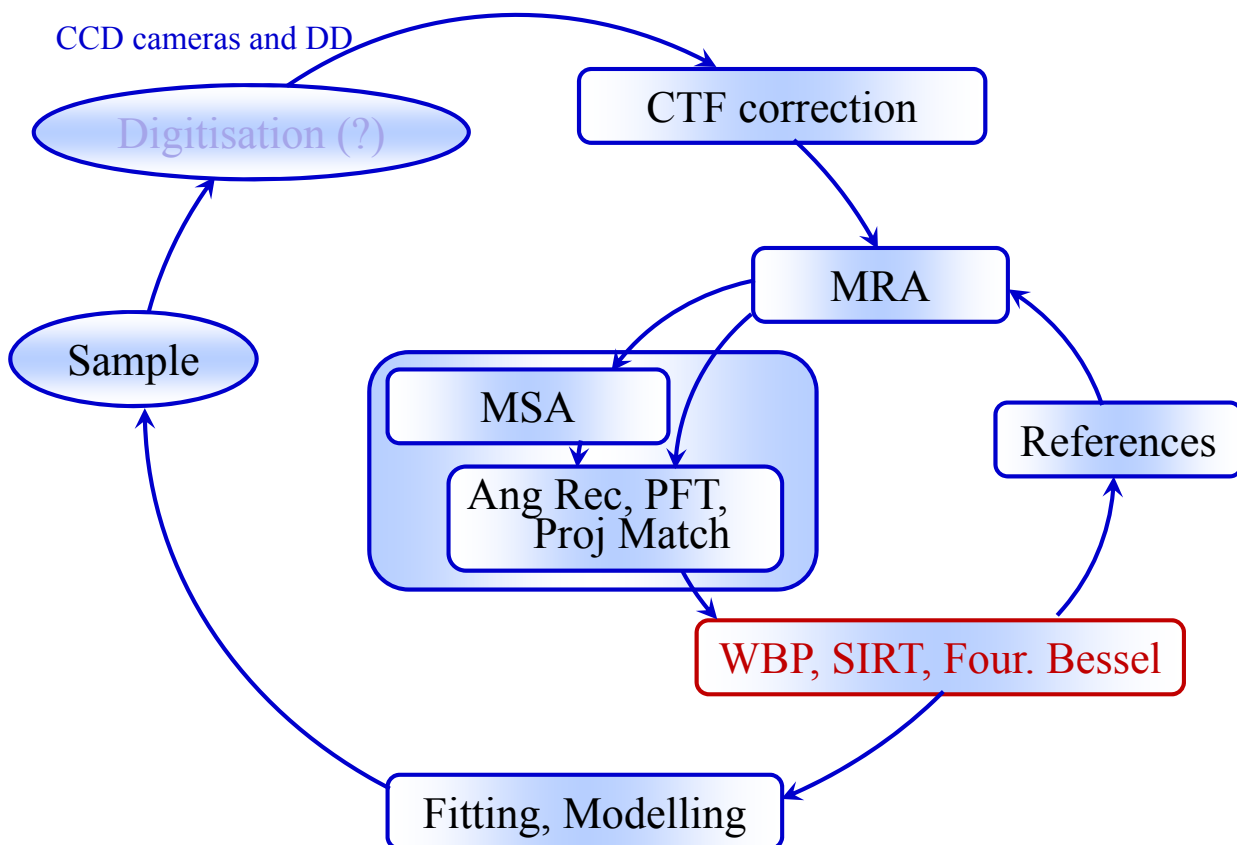
## Introduction



## Where do we stand now?



## Which processing is essential?



# Three dimensional reconstruction of objects from their projections

Two-dimensional projection from three-dimensional object

$$p(y, z) = \int \rho(x, y, z) dx$$

Medical X-ray images, Ultra sound images, EM images may be considered as 2D projections of objects

One-dimensional projection from two dimensional object

$$l(y) = \int p(x, y) dx$$

Medical X-ray scans present 1D projections of the object

## Medical X-ray images

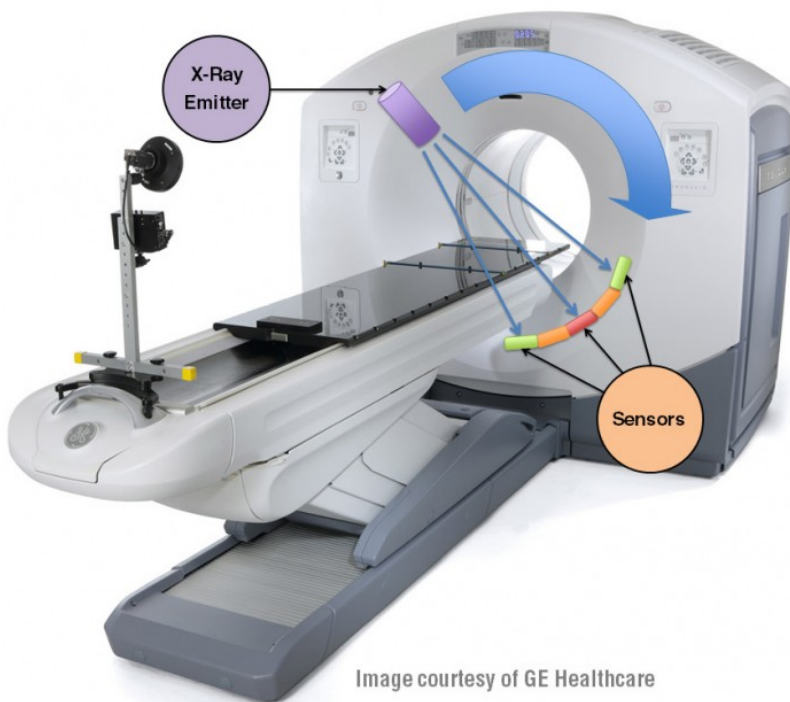
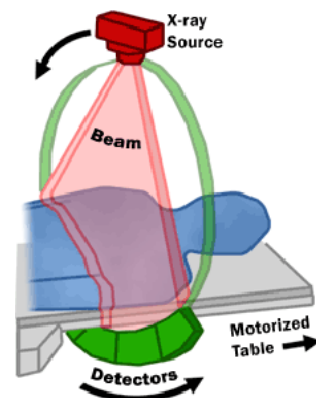
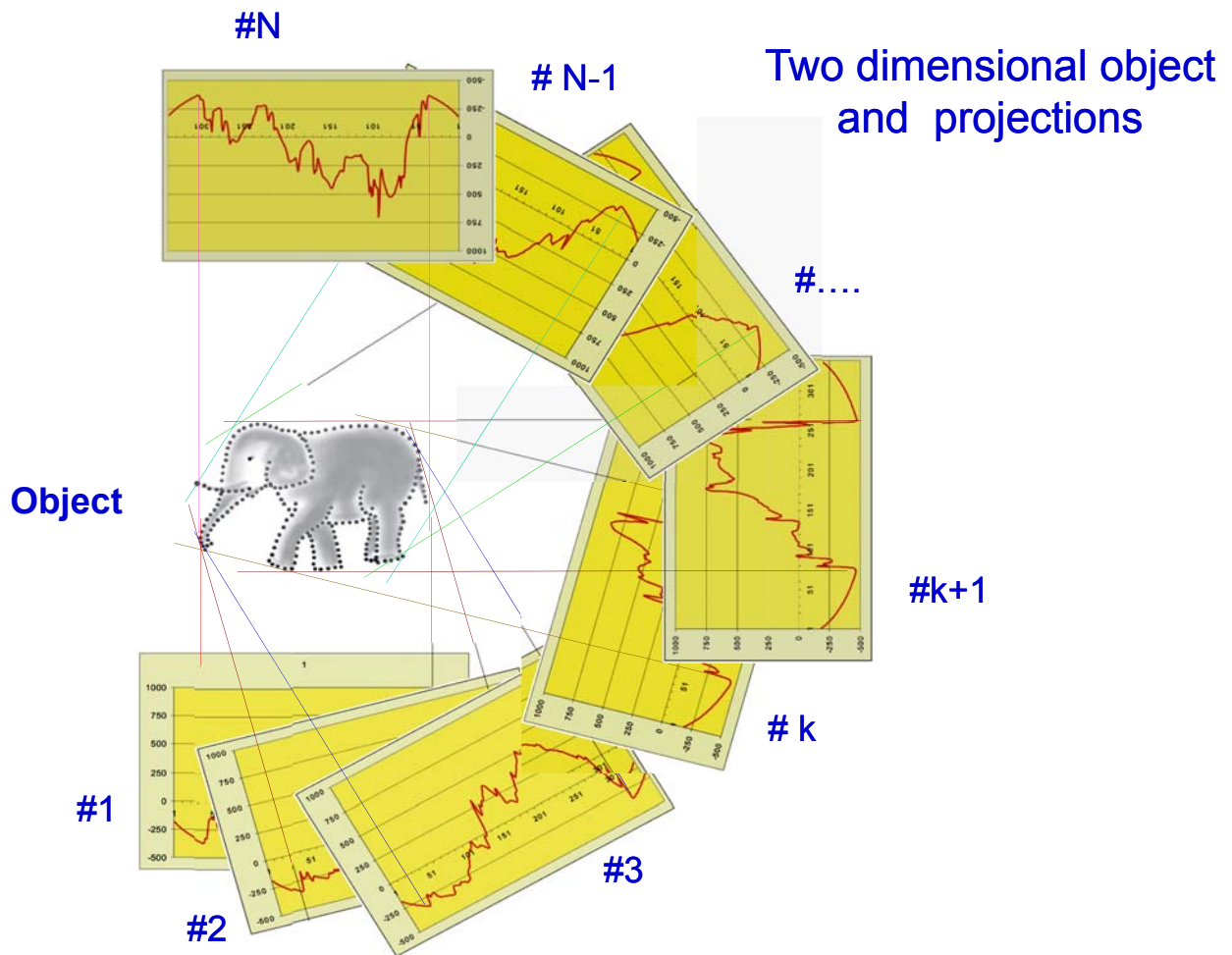
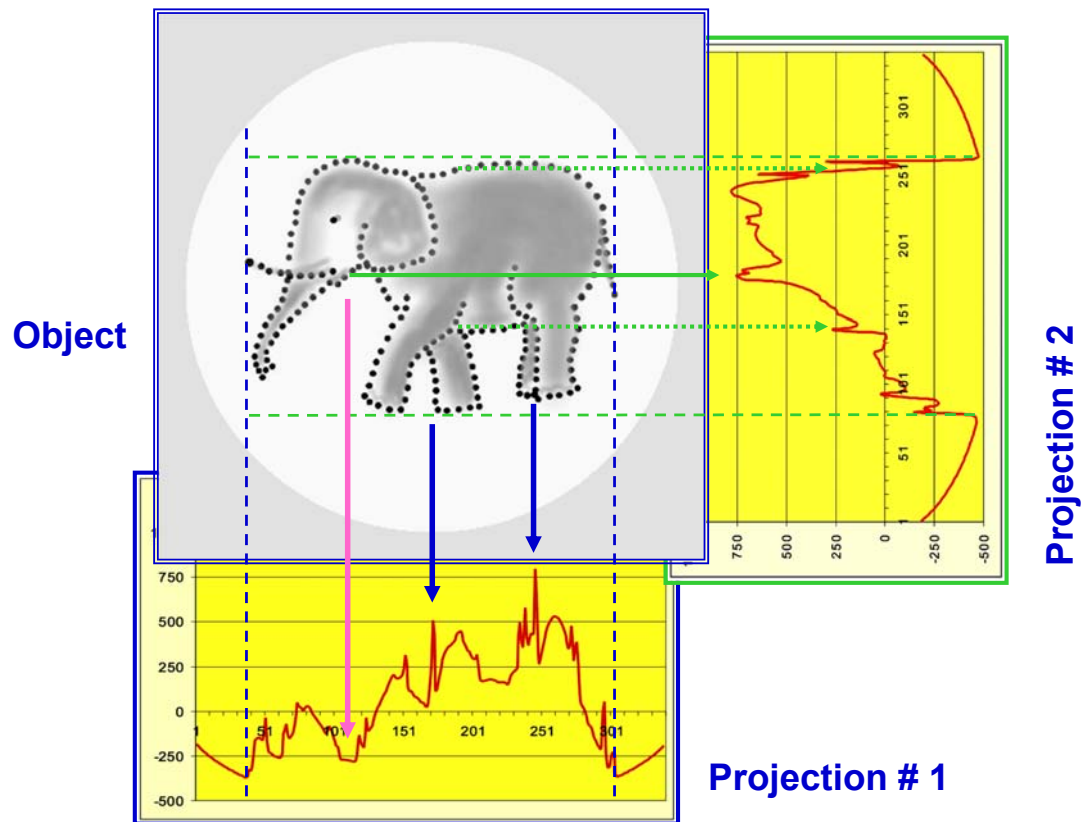


Image courtesy of GE Healthcare



# Two dimensional object and projections



Here is a reversed problem:

***How from projections can be restored  
three-dimensional distribution of densities?***

It has been shown by J. Radon (Germany) in 1917 that it is possible to restore 3D distribution of densities using a continuous set of 1D projections. The operation obtained a name:

**REVERSED RADON TRANSFORMATION**

J. Radon has demonstrated a theoretical solution of the problem. A practical realization of the solution came much later and for the first time in medical tomography. Then some methods were developed in astrophysics. Electron microscopy started to develop methods in later 70<sup>th</sup>.

**Why people do not use  
the analytical result obtained by Radon?**

1. All samples both in medicine and electron microscopy are very sensitive to the penetrating radiation. Therefore it is impossible to take a large number of images. **We do not have a complete continuous set of projections.**
2. **A range of angles** where projections are obtained **does not cover the Euler sphere completely.**
3. In medical tomography the X-Ray beam is not parallel.

**Electron microscopy has some advantages :**

- In vitrified samples molecules are oriented very often randomly and therefore possible orientations can cover Euler sphere rather evenly.
- Some molecules have symmetry that can be used.

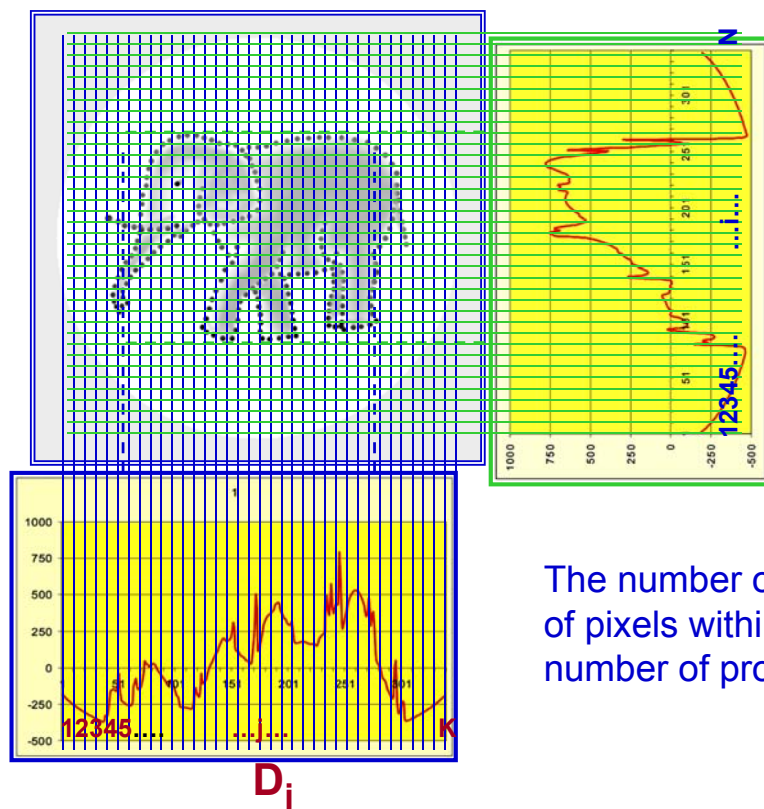
# Part 1

## Algebraic reconstruction methods

### Back projection

### Filtered back projection – - convolution method

## Algebraic reconstruction methods



K - number of pixels in horizontal direction

N - number of pixels in vertical direction

j - column index

i - row index

$$D_j = \sum_{i=1}^N x_{ij}; \quad 1 < i < N \\ 1 < j < K$$

Number of unknown density pixels  $X_{ij} = N \times K$

The number of equations is the number of pixels within the projection times the number of projections

# Algebraic Reconstruction Technique

$$\Delta x_j^{(i)} = x_j^{(i)} - x_j^{(i-1)} = \frac{d_i - p_i}{\sum_{k=1}^N w_{ik}^2} w_{ij}$$

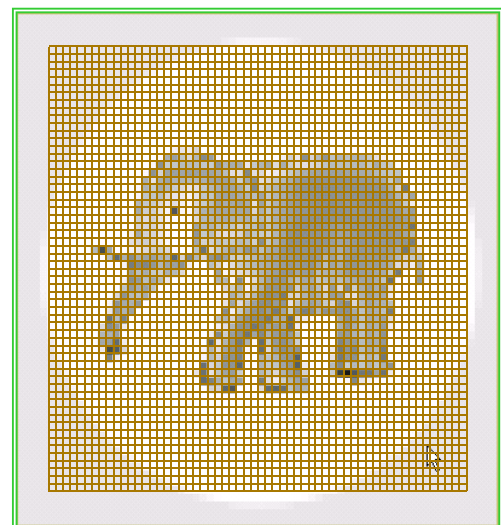
- $d_i$  – measured projection density
- $p_i$  – calculated projection density
- $x_i$  – estimated projection density
- $w_{ij}$  – weight of the pixel : 1 or 0

# Simultaneous Iterative Reconstruction Technique

SIRT –was proposed by Gilbert in 1972. Estimated densities are corrected using the discrepancy between all real and estimated projections in one round.

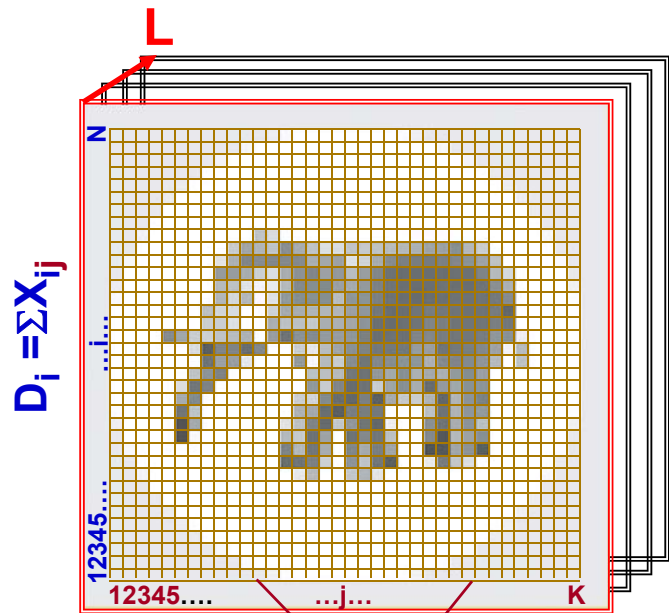
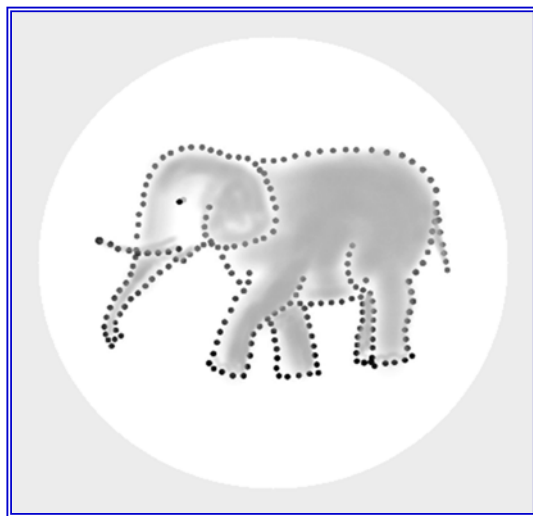
$$\Delta x_j^{(i)} = \frac{1}{M} \sum_{i=1}^{i=M} \frac{d_i - p_i}{N_i}$$

For the cube with the size of 100 pixels the number of voxels is  $100^3$ . The number of projections is in the best case  $\sim 2000$ . Very often it is much less. The exact solution is impossible, though iterative methods are able to find an approximate solution.



The methods give fast and reasonable solution if there are only few projections, or it will be a two-dimensional problem

# Algebraic reconstruction methods



The number of unknowns ( $N \times K \times L$ ) in the set of equations is the number of voxels in the object ( $L$  = number of slices through the object).

$$D_j = \sum X_{ij}$$

# Algebraic reconstruction methods

The Algebraic Reconstruction Technique (ART), developed by R. Gordon (A tutorial on ART, 1974, IEEE Trans. NS-21, 78-93). The principle of the algorithm is based on iterative refinement of the initial estimation of  $X_{ij}$  using comparison calculated reprojections with real projections. The difference between them is used to modify values of  $X_{ij}$ .

## Additive

methods –  
correction of density estimation by adding differences between real and estimated projections

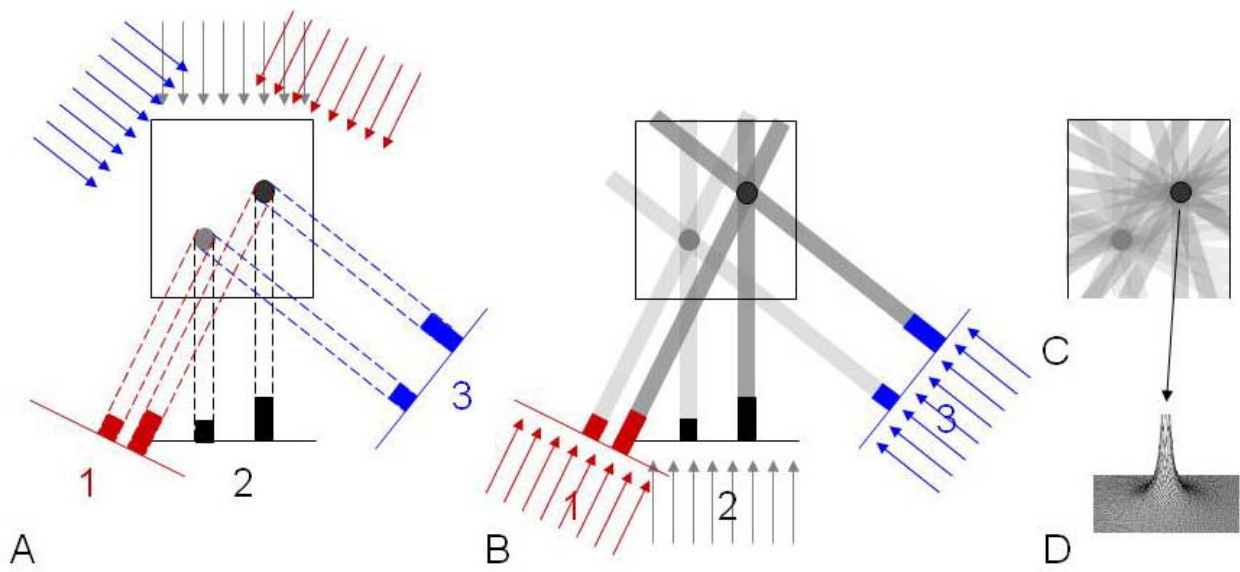
## Multiplicative

methods –  
correction of density estimation by calculation of correction coefficients for estimated projections

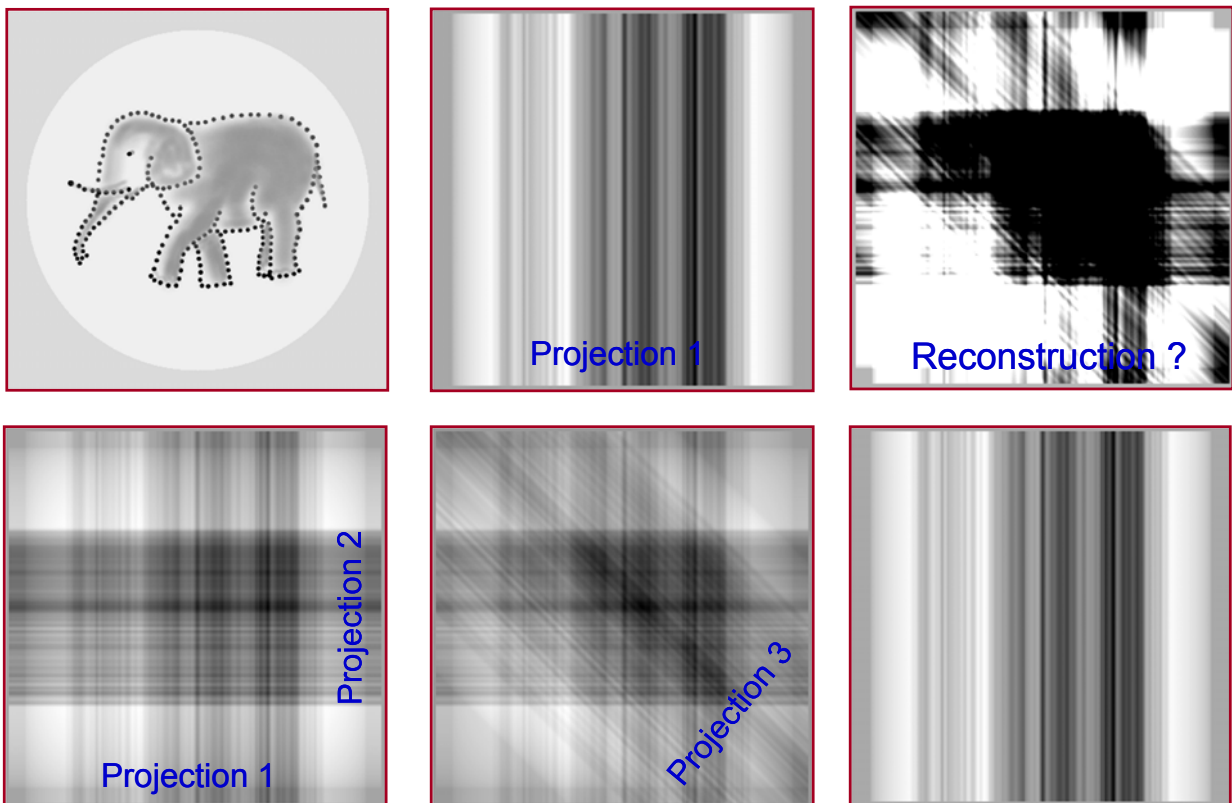
## Iterative relaxation

methods –  
estimation of density has to satisfy a number of conditions.

# Back projection



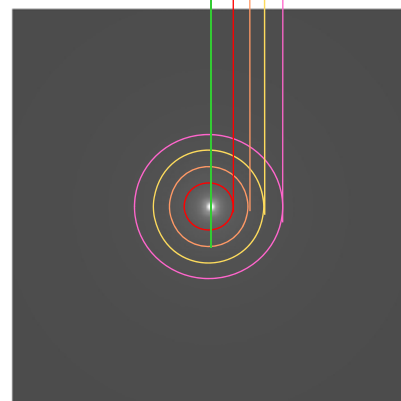
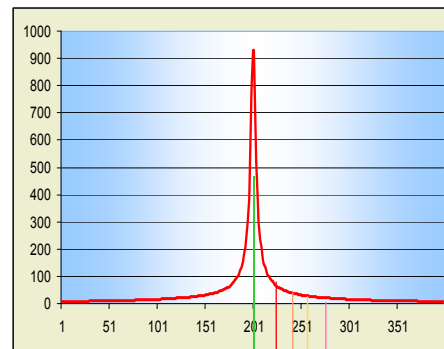
# Back projection



## Back projection

The simplest algorithm has one serious limitation.

If we are reconstructing only one point, it will be surrounded by background that is proportional to  $1/r$ , where  $r$  is the distance from the point. That background is proportional to intensity of the local point. It makes the whole reconstruction smeared.



Point spread function

Estimation of reconstruction using back projection can be presented as convolution of the object function with  $1/r$  function for two dimensional and with  $1/r^2$  for three dimensional object.

$$\rho_{est}(\mathbf{r}) = \rho(\mathbf{r}) \otimes (1/r) \quad \text{for 2D}$$

$$\rho_{est}(\mathbf{r}) = \rho(\mathbf{r}) \otimes (1/r^2) \quad \text{for 3D}$$

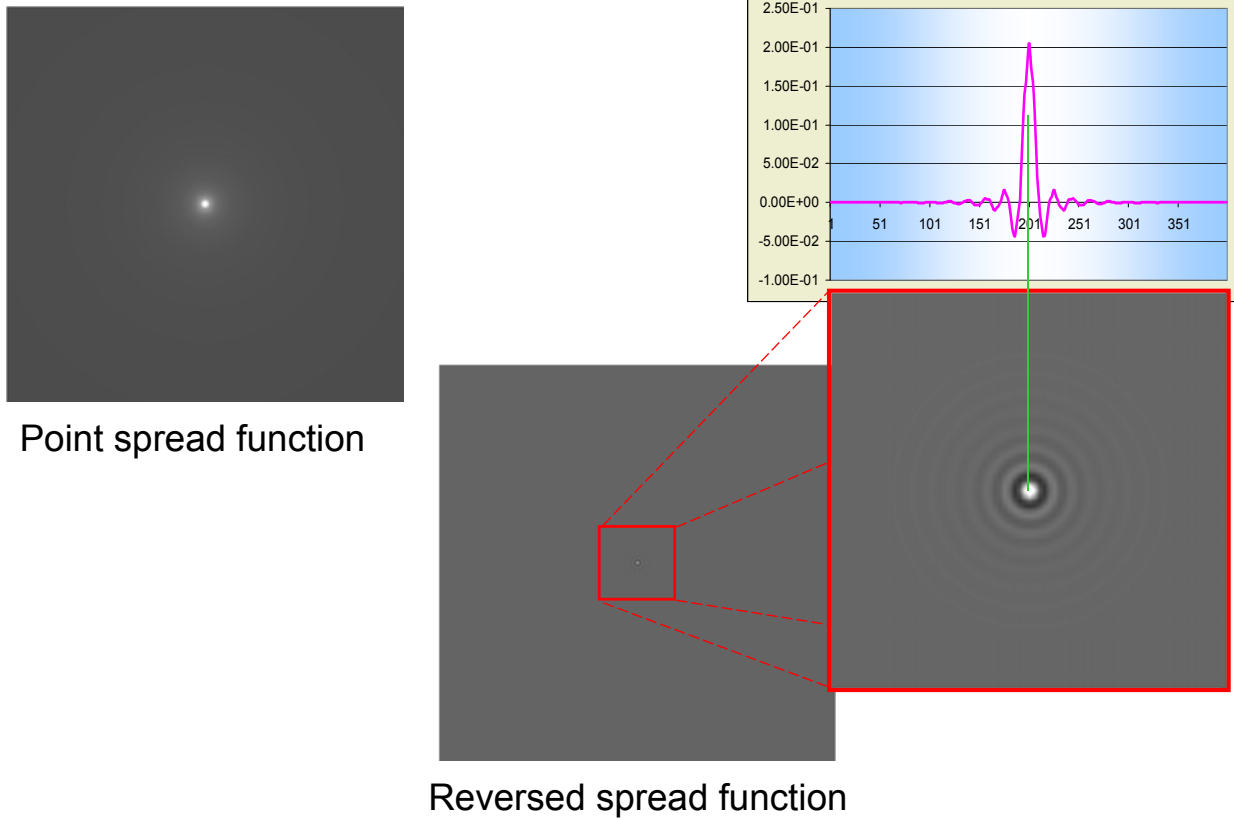
where  $\otimes$  is the convolution operator

A general approach of solving the problem is finding of a new function  $\mathbf{F}_{filt}$  that will change the projections in such way, that reconstruction will give a good estimation of  $\rho(\mathbf{r})$

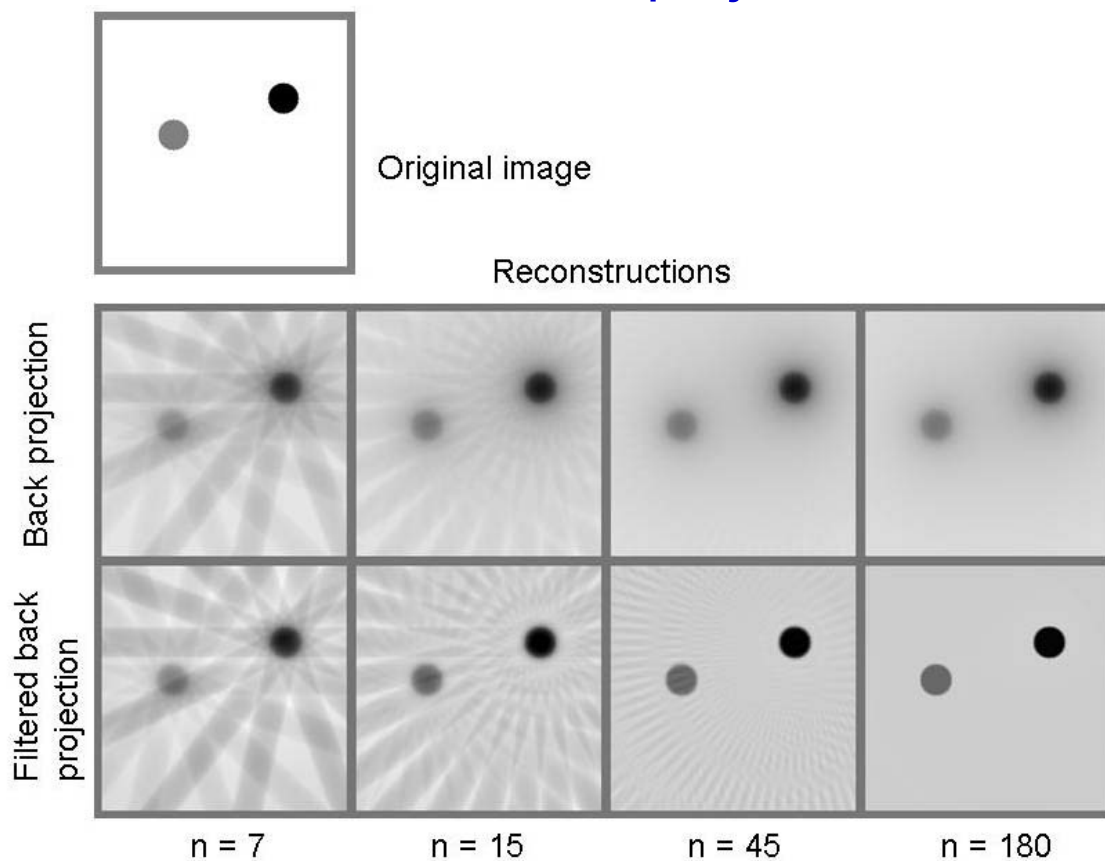
$$\rho_{est}(\mathbf{r}) = \int_0^{\pi} [p'(l, \alpha) \otimes \mathbf{F}_{filt}(l)] d\alpha$$

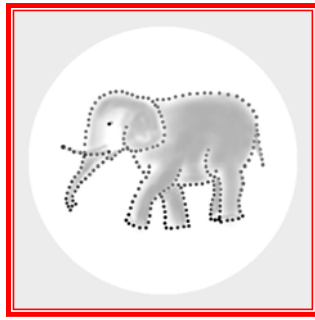
There are several approximation of the function  $\mathbf{F}_{filt}$  and one of them is R filtering of back projections.

## Back projection. How to overcome problems?

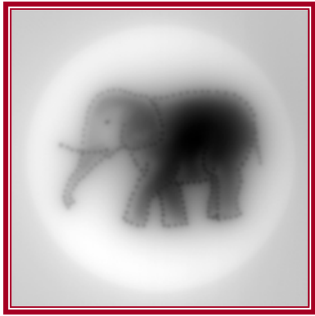


## Filtered back projection

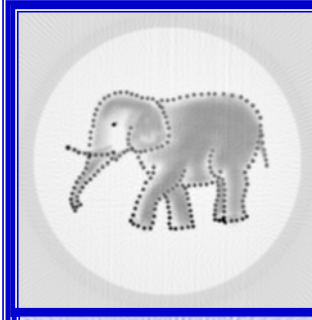




Object

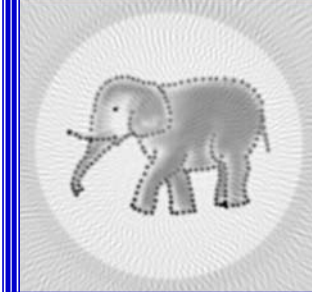


Back projection  
180 projections

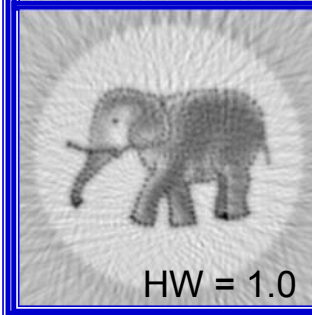


Filtered back projection

180 projections, equally distributed  
HW (Hamming window) = 1.0

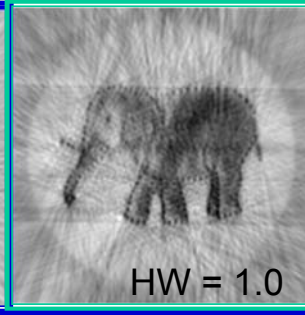


90 projections, equally distributed  
HW = 1.0

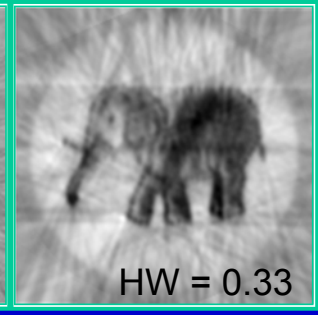


36 projections

Randomly distributed projections



HW = 1.0



HW = 0.33

## Part 2

### Fourier methods, Fourier-Bessel functions

#### Reconstruction in frequency space = Fourier methods

The principle of the method is based on calculation Fourier transforms from projections, taken in many different directions. Since they correspond to the central sections of 3D Fourier transform, it is possible to recover a whole 3D transform. The reverse Fourier transform will provide distribution of densities within the object.

Fourier transform of the object  $r(x,y,z)$

$$\mathcal{F}(X,Y,Z) = \iiint r(x,y,z) \exp(-2\pi i(xX + yY + zZ)) dx dy dz$$

Central section of the Fourier transform is a section through the origin of the system. Let us guess, that it will be the plane XY

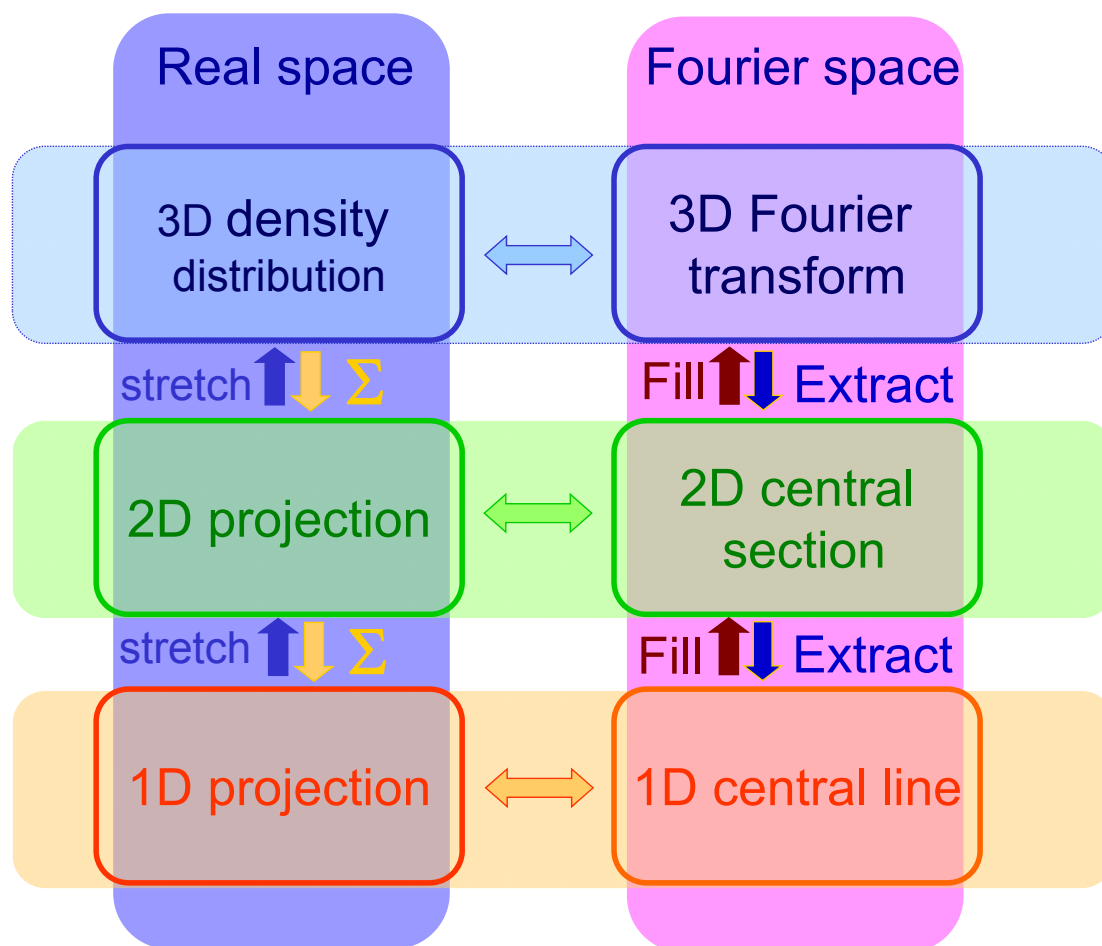
$$\mathcal{F}(X,Y,0) = \iiint r(x,y,z) \exp(-2\pi i(xX + yY + z0)) dx dy dz$$

$$\mathcal{F}(X,Y) = \iiint r(x,y,z) \exp(-2\pi i(xX + yY)) dx dy dz$$

$$p(x,y) = \int r(x,y,z) dz$$

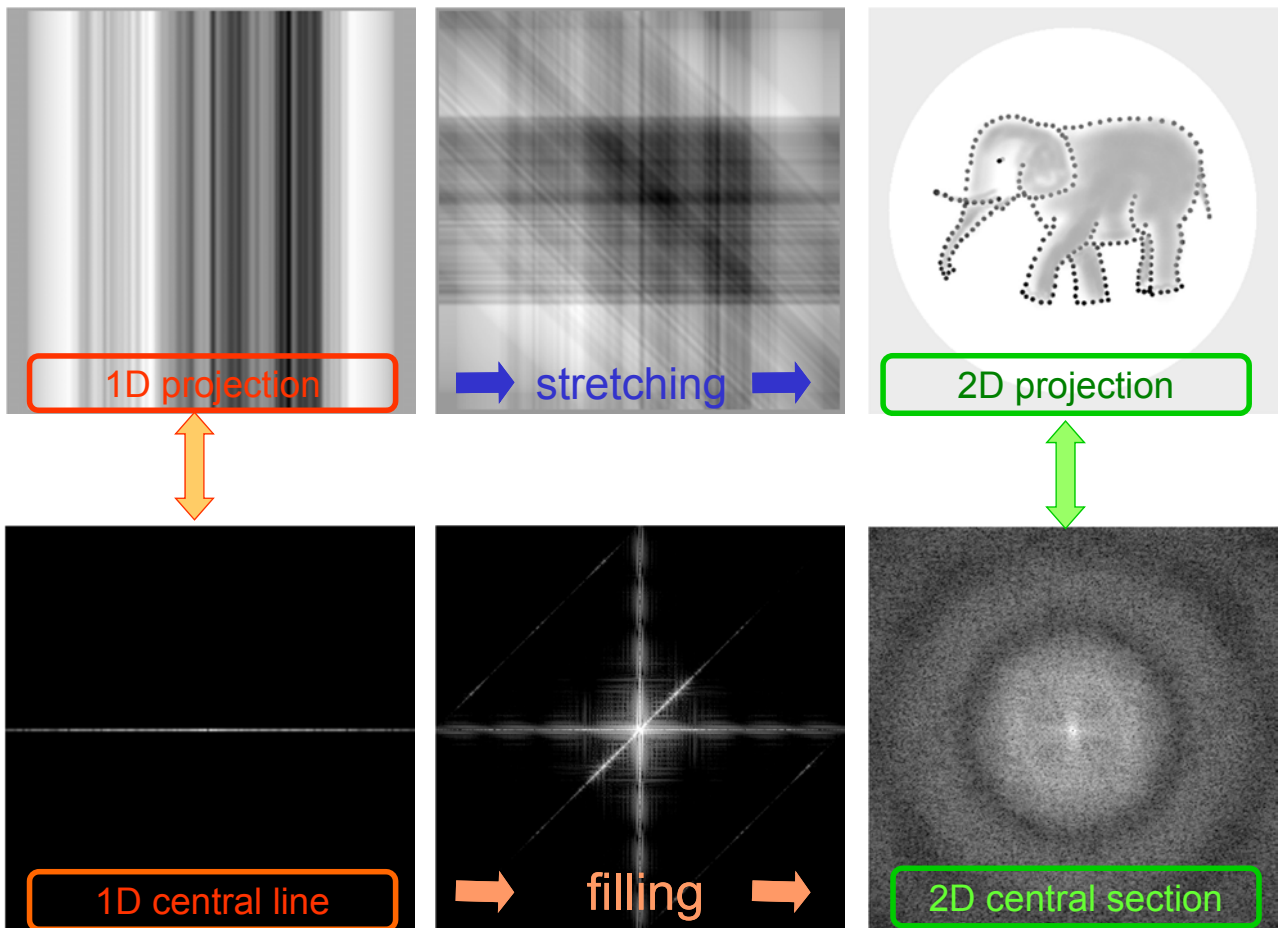
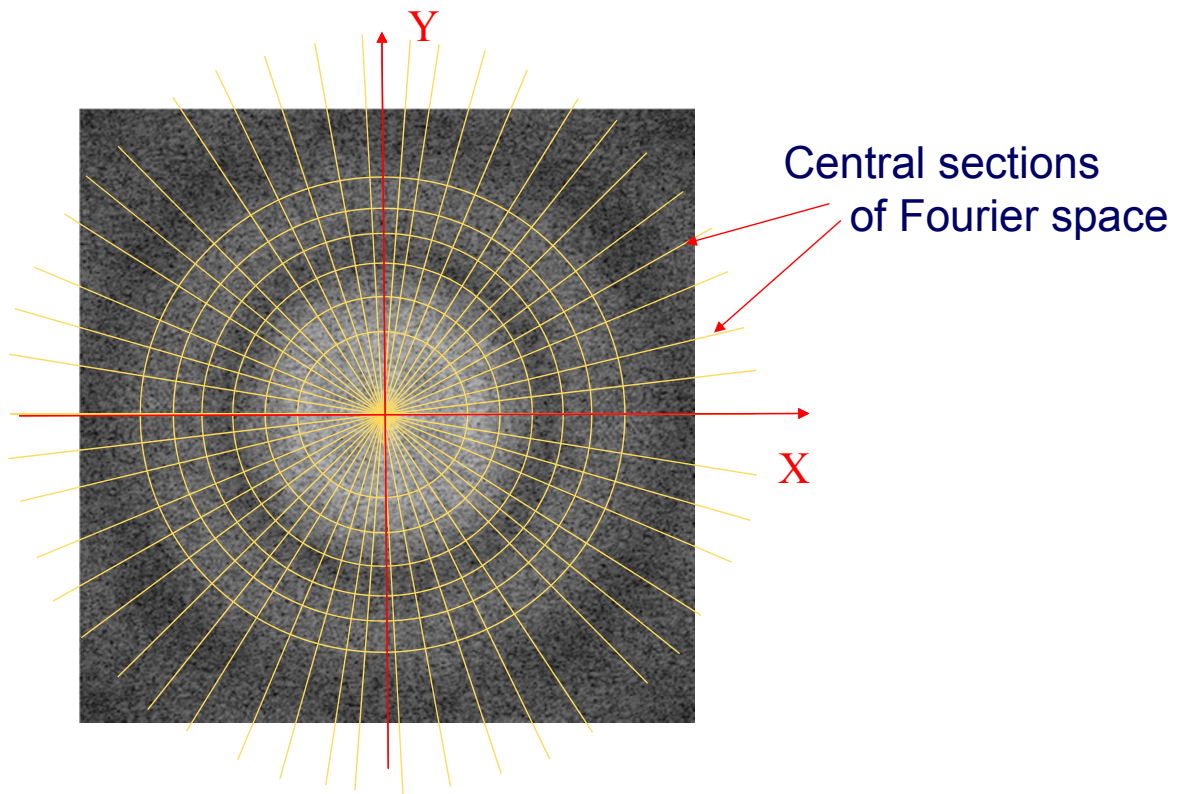
However, the result of this integration corresponds to the projection of the object on the plane xy

$$\mathcal{F}(X,Y) = \iint p(x,y) \exp(-2\pi i(xX + yY)) dx dy$$

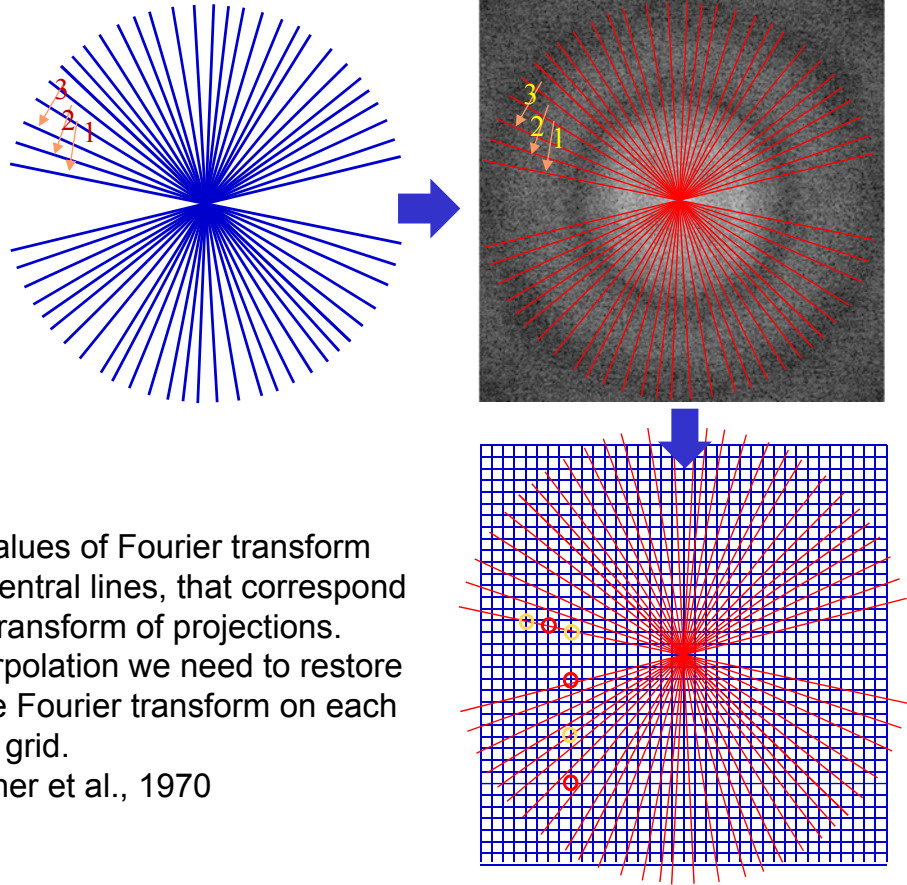


# Fourier methods

$$\mathcal{F}(X, Y) = \iint p(x, y) \exp(-2\pi i(xX + yY)) dx dy$$

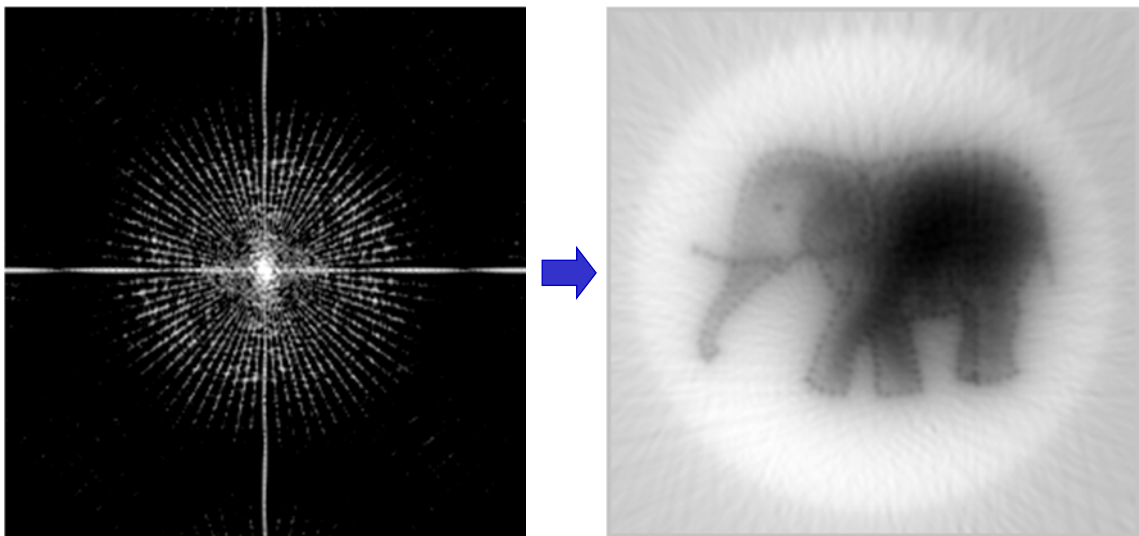


## Fourier methods

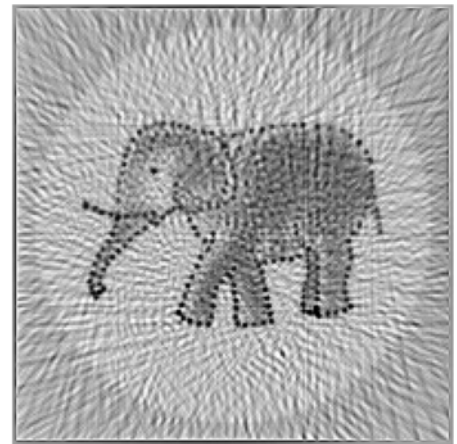
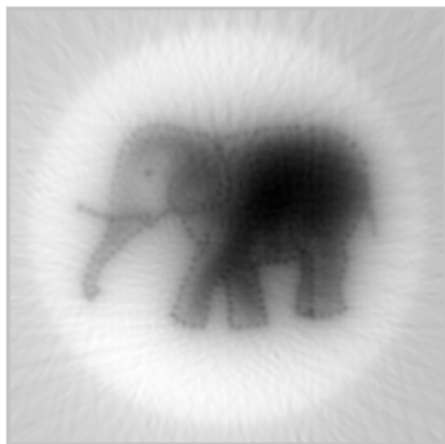
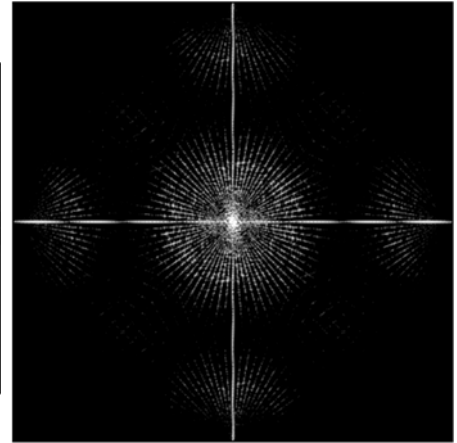
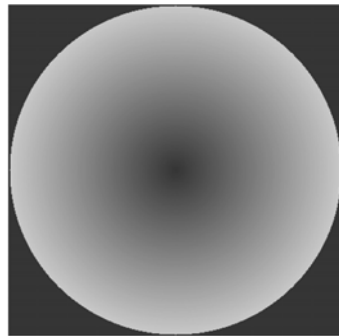
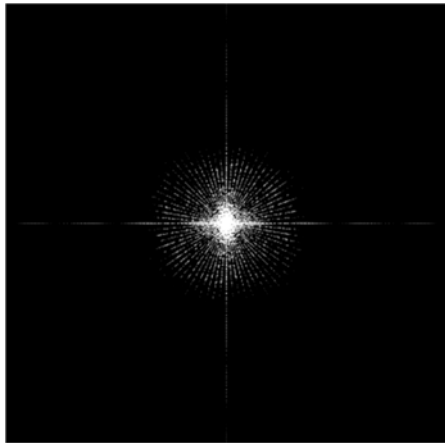
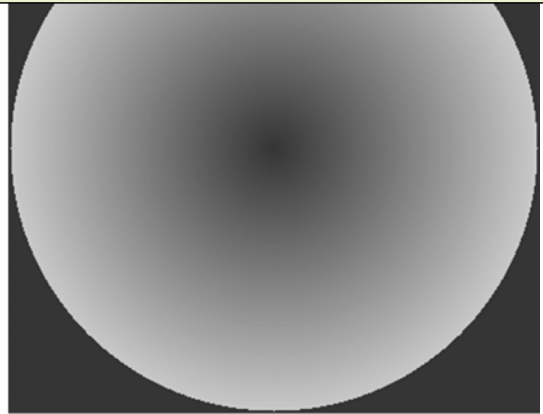
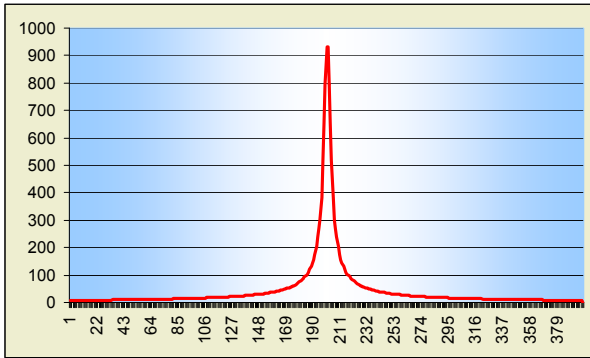


We have values of Fourier transform along the central lines, that correspond to Fourier transform of projections. Using interpolation we need to restore the discrete Fourier transform on each pixel of the grid. See Crowther et al., 1970

## Reconstruction in frequency space = Fourier methods



# Fourier methods



## Part 3

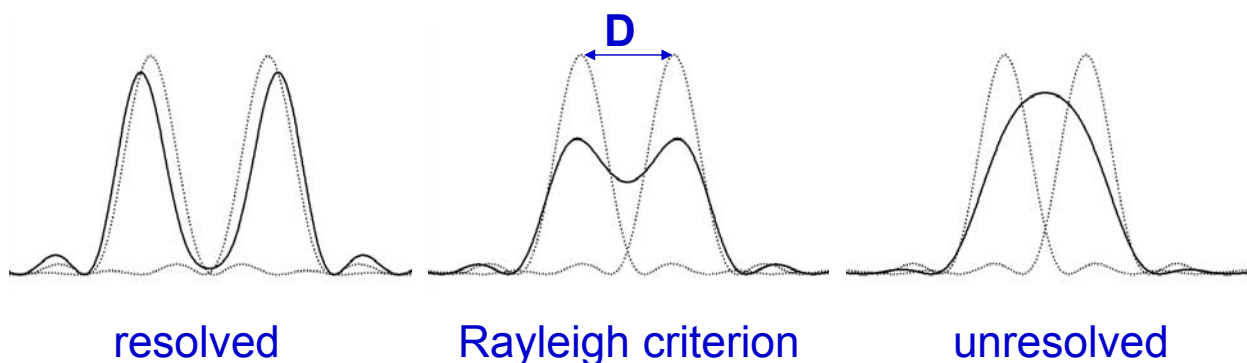
### Evaluation of quality of 3D reconstructions A resolution criterion

A final result of image analysis of single particles will be a three dimensional map of density distribution.

How can we check the size of details which are reliable and which reflect noise ? The minimal size of reliable details is used to indicate the resolution of the reconstruction obtained.

We can compare two structures by calculating their correlation. However CCF is not sensitive to the fine details, it depends mainly on the large details and on the shape of the molecule. In crystallography it is common to use Fourier space to evaluate the resolution of the structure where resolution is specified by the distance of the highest order reflections from the central peak.

### Evaluation of resolution in images

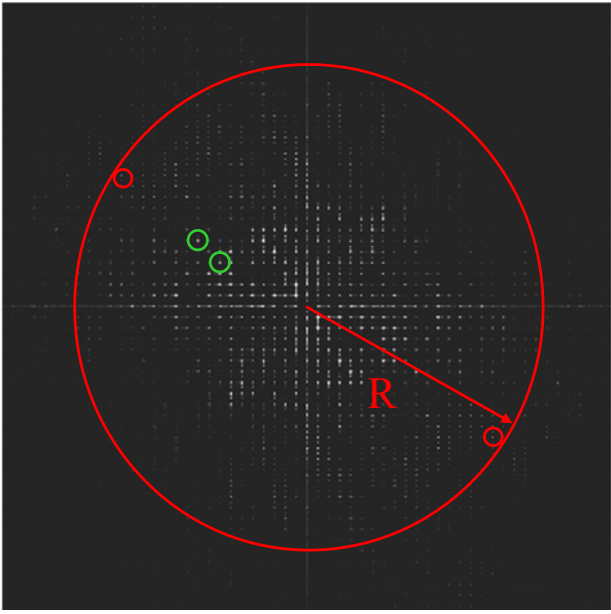
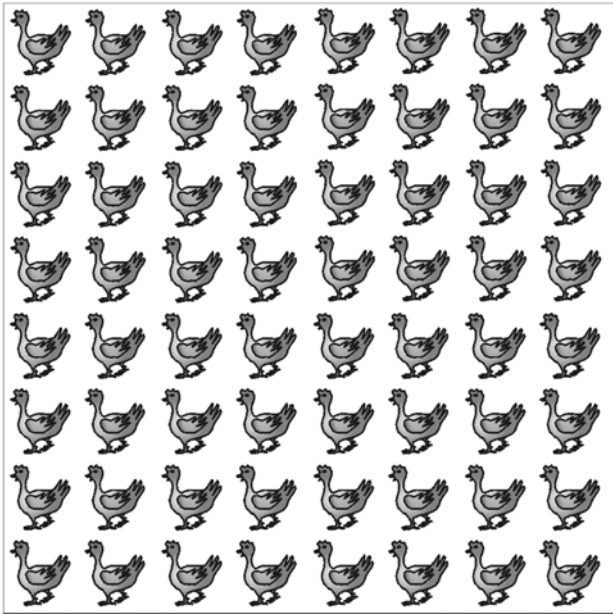


When the separation distance (**D**) between adjacent Airy patterns is greater than the central disk radius (**r**), the sum of the intensities yields two individual peaks. As the disks approach each other, the separation distance will reach a value equal to the central disk radius, a condition known as the Rayleigh criterion. At even closer approach, the separation distance is less than the central disk radius and the sum of the two peaks merges into a single peak. In the latter instance, the two Airy patterns are said not to be resolved.

$$\text{Sin} (\Theta_R) = 1.22 \lambda / d ,$$

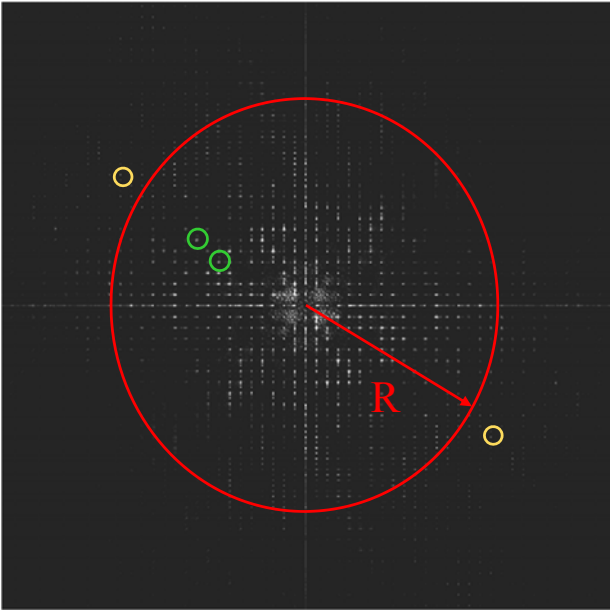
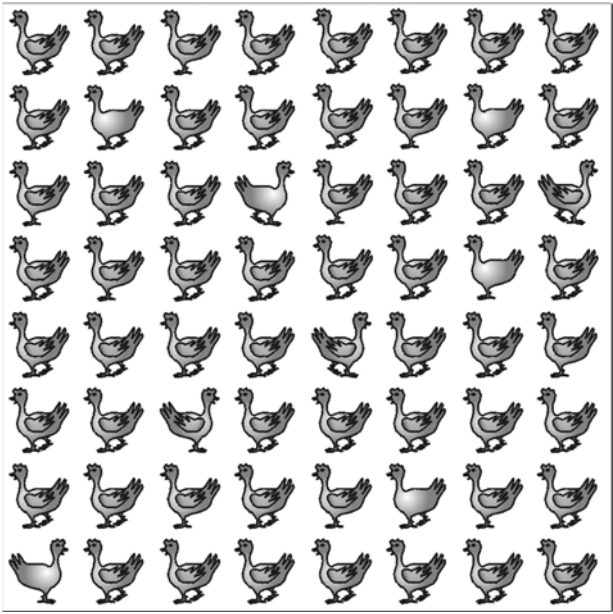
where  $D = \text{Sin} (\Theta_R)$ ;  $\lambda$  – wave length;  $d$  – aperture of the imaging system

# Evaluation of resolution in crystallography



Resolution =  $1/R$ , where R is a spatial frequency

# Evaluation of resolution in crystallography



However, a 3D reconstruction of the single molecule does not have any periodicity. That makes impossible distinguishing signal and noise in the Fourier spectrum from one reconstruction. It was suggested to compare Fourier spectra of several independent reconstructions.

**SSNR - Spectral signal-to-noise ratio** (Steven et al, S2/N2)

The approach is statistical analysis of spectra of several reconstructions (Unser, M. *et al.*, 1987).

The other which is more popular compares spectra of two independent reconstructions. There are following criteria used more often to evaluate their similarity :

1. Fourier ring correlation (van Heel, Saxton and Baumeister)

**Cross-correlation coefficient (single particle)**

plot out full curve

resolution at 0.5 cross-correlation

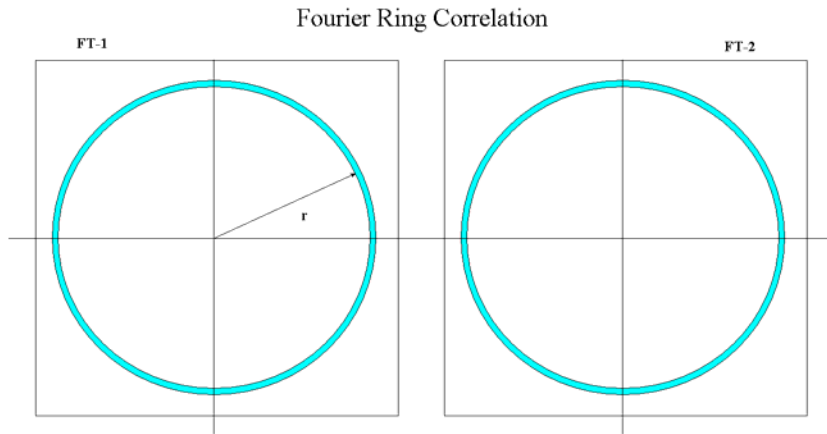
resolution at 3\*sigma (noise)

interpretable at 0.15 cross-correlation, unless overfitted

2. The differential phase residual ( J. Frank) **Phase residual (2D crystal & single particle)** each measurement vs. average of all comparable divide data into two halves, average and plot difference

$$\overline{\Delta\phi}(k, \Delta k) = \left| \frac{\sum_{[k, \Delta k]} [\Delta\phi(\mathbf{k})]^2 [ |F_1(\mathbf{k})| + |F_2(\mathbf{k})| ]}{\sum_{[k, \Delta k]} [ |F_1(\mathbf{k})| + |F_2(\mathbf{k})| ]} \right|^{1/2}$$

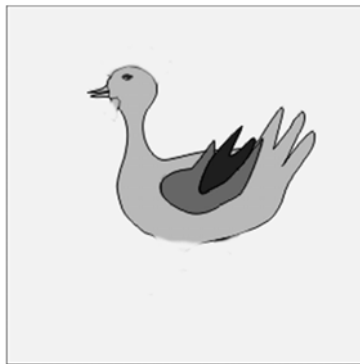
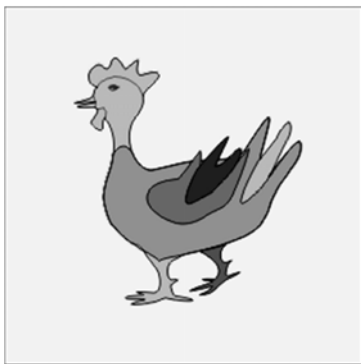
# Fourier Ring/Shell Correlation



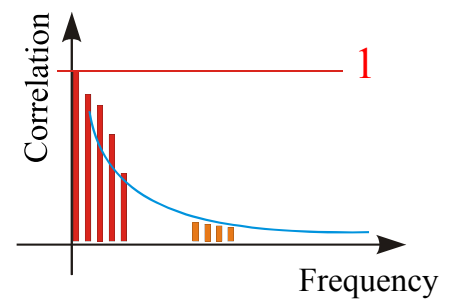
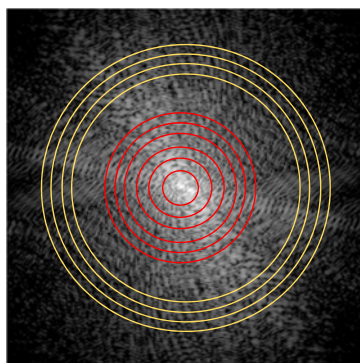
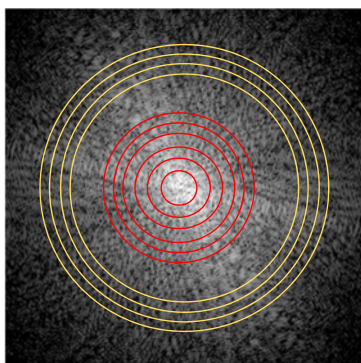
$$FSC_{12}(r_i) = \frac{\sum_{r \in r_i} F_1(r) \cdot F_2(r)^*}{\sqrt{\sum_{r \in r_i} F_1^2(r) \cdot \sum_{r \in r_i} F_2^2(r)}}$$

**Saxton & Baumeister  
(1982)**

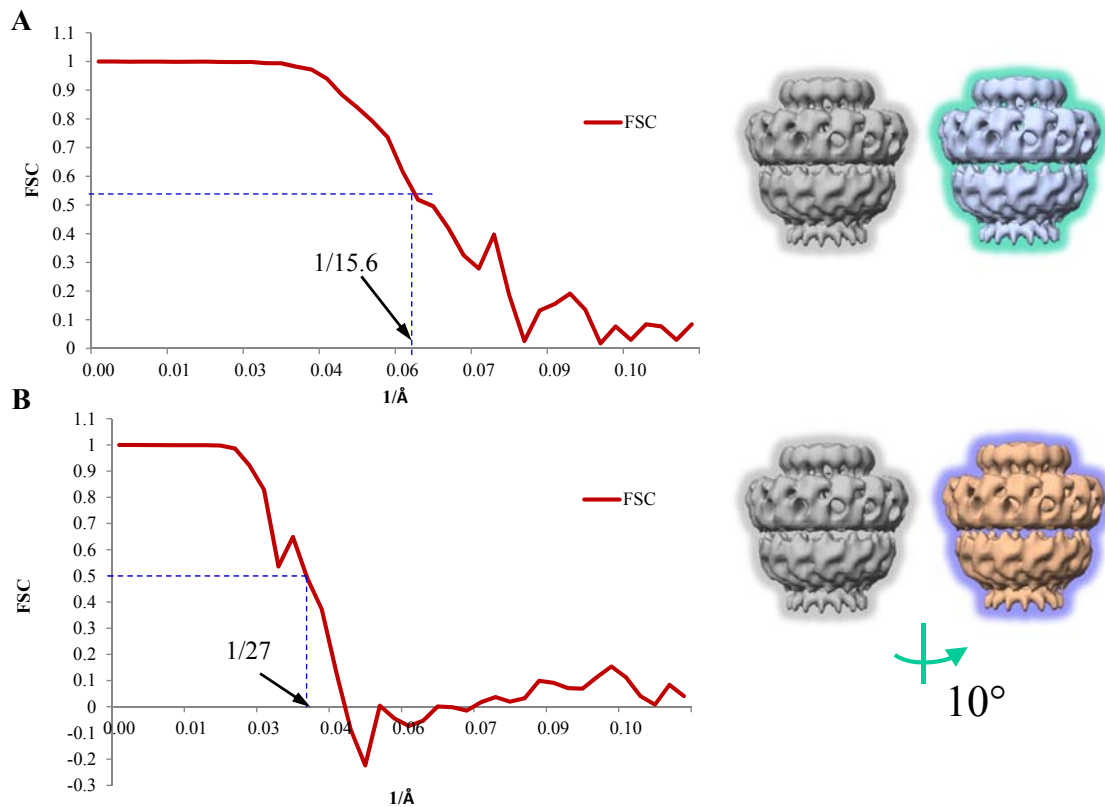
**Van Heel et al. (1982)**



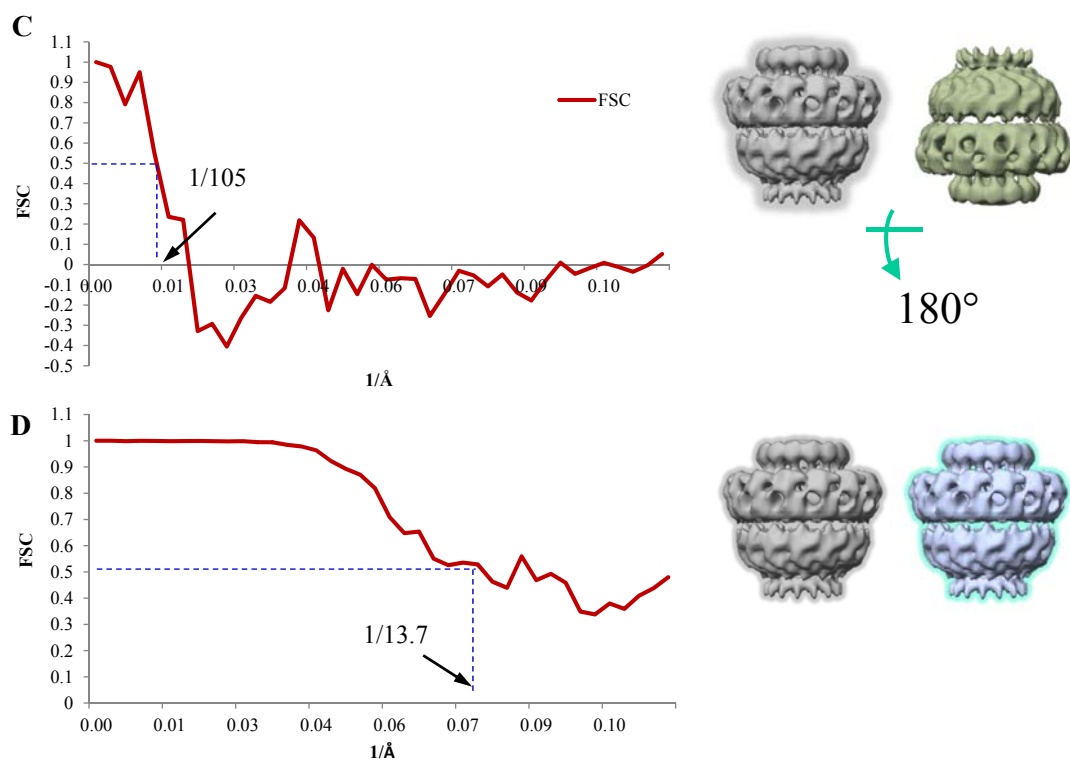
Fourier ring  
correlation



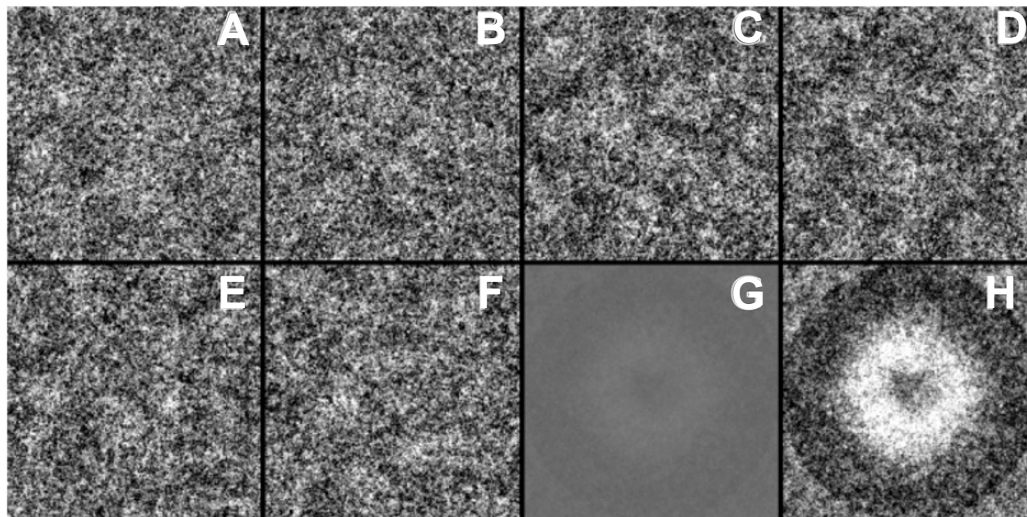
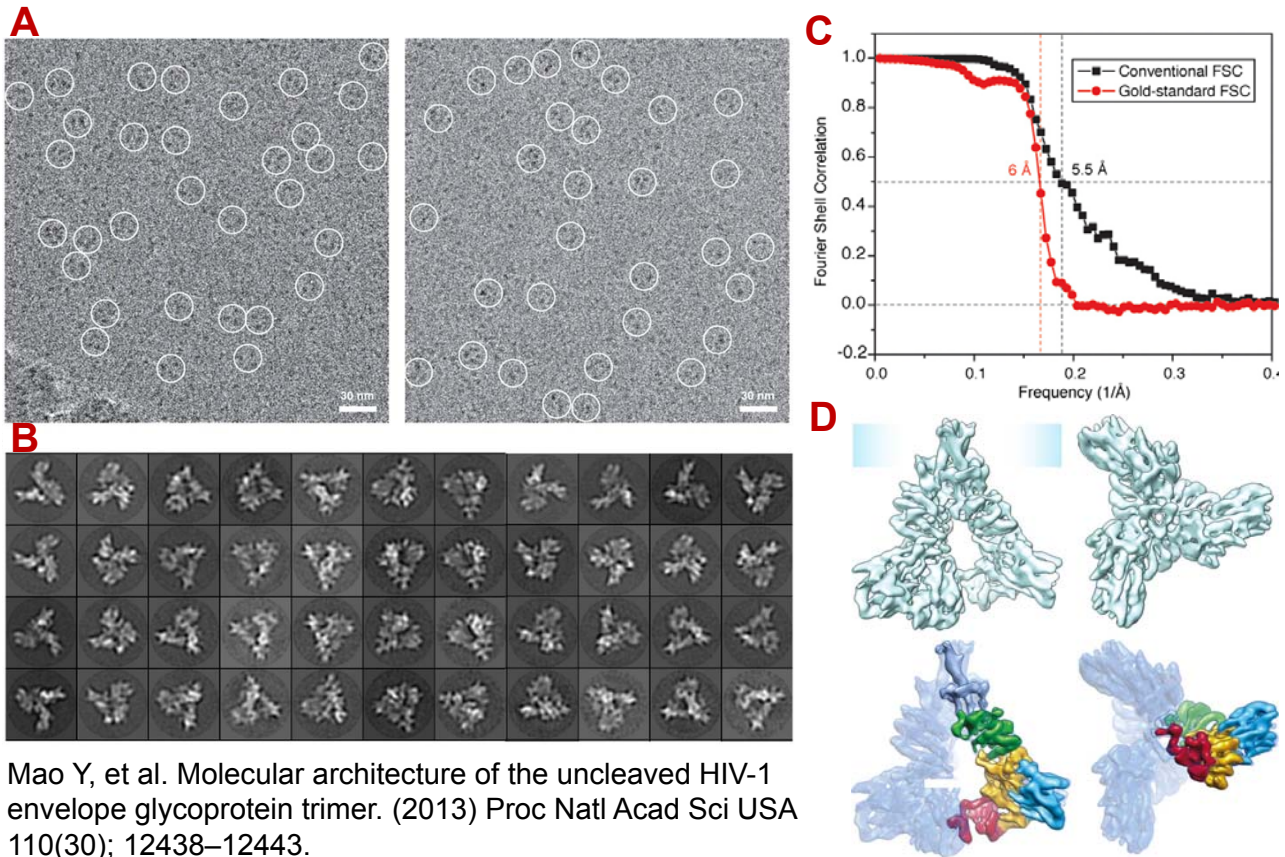
## Fourier Shell Correlation and its features



## Fourier Shell Correlation and its features

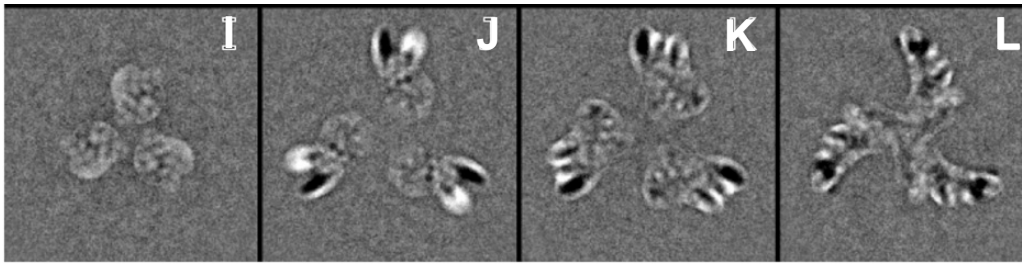


## Overzealous attempts to get a high resolution structure and problems related



- (A–F) Individual images of particles from the stack of 423 (21).  
 (G) Average of 423 windowed images using the same grey scale as A–F.  
 (H) Average of 423 windowed images with increased contrast. The density in the central region of G and H shows the average of the many views used in particle picking. The circle of dark density round the edge of the average, seen more clearly in H should not be present in the raw images so must arise from masked projections from the 3D map or model used to extract the particles.

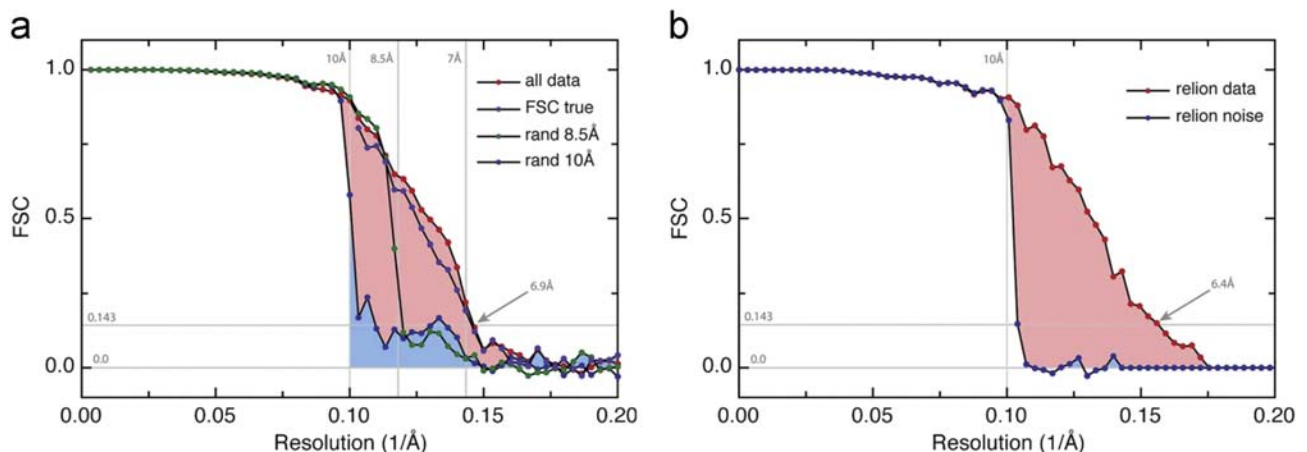
Henderson R. Avoiding the pitfalls of single particle cryo-electron microscopy: Einstein from noise (2013) Proc Natl Acad Sci U S A. Nov 5;110(45):18037-41



(I–L) Difference maps obtained by **subtraction of sections from the two independent half maps** [i.e., maps calculated using only half the data, normally even and odd particles in the stack (18)] supplied by the authors (21). The four panels represent sections at different heights along the spike, viewed from the apex. The differences are confined to a sharply defined region with no gradation into the flat background. This clearly visible and relatively sharp mask serves to constrain any density to the region inside the mask during iterative refinement. Use of masking plus the same initial reference suggests how the apparent resolution was extended from 11 to 6 Å. All images are on the same scale, with a window size of 190 Å.

Henderson R. Avoiding the pitfalls of single particle cryo-electron microscopy: Einstein from noise (2013) Proc Natl Acad Sci U S A. Nov 5;110(45):18037-41

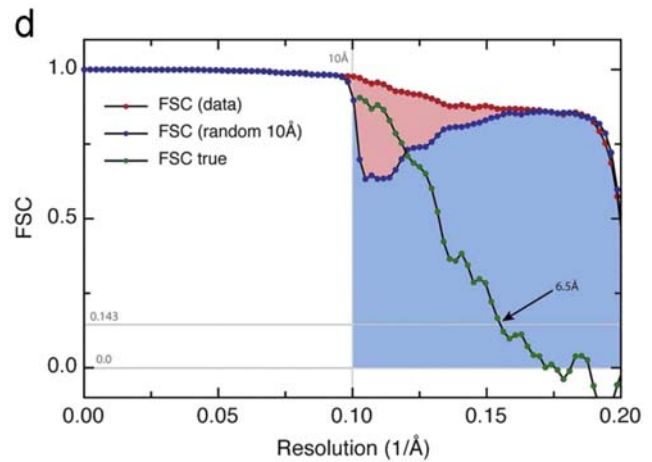
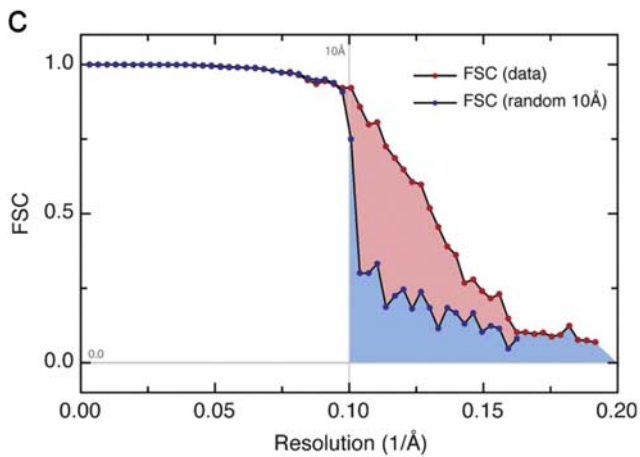
## Validation of 3D cryoEM maps



~44,000 single particle images of  $\beta$ -galactosidase (300 keV, FEI Falcon II detector) using four different procedures. The FSC from the particle data set (red) is compared in each case with that obtained from the same data set with HR-noise substituted beyond 10 Å (blue).

(a) Data out to 7 Å resolution was used in orientation determination, so the overfitting is only evident between 10 and 7 Å resolution. In this case, the very small degree of overfitting does not affect the estimated resolution. (b) Gold-standard FSC weighting was used with low-pass filtering of the reference at each cycle as described. There is no overfitting, confirmed by values of  $FSC_n$  that are zero beyond 10 Å. The map shows 6.4 Å resolution. (Chen et al, Ultramicroscopy, 2013)

## Validation of 3D cryoEM maps



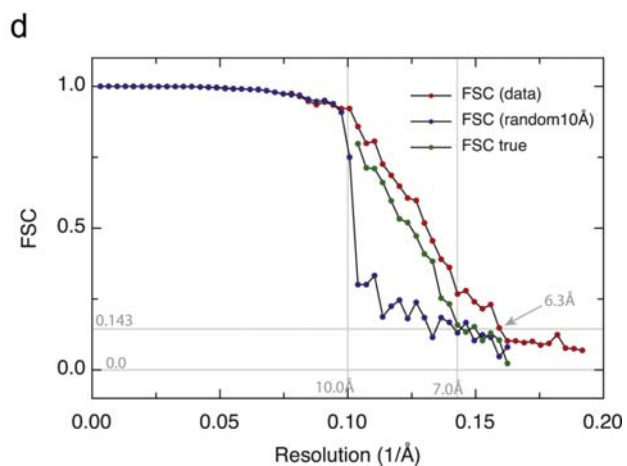
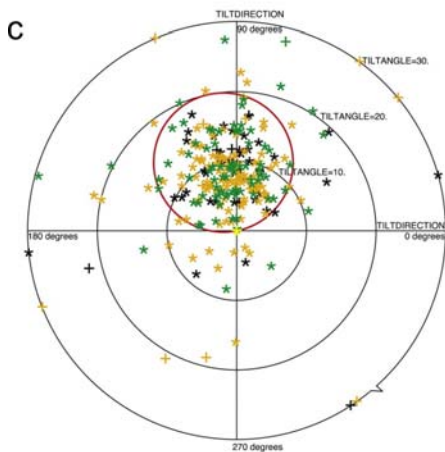
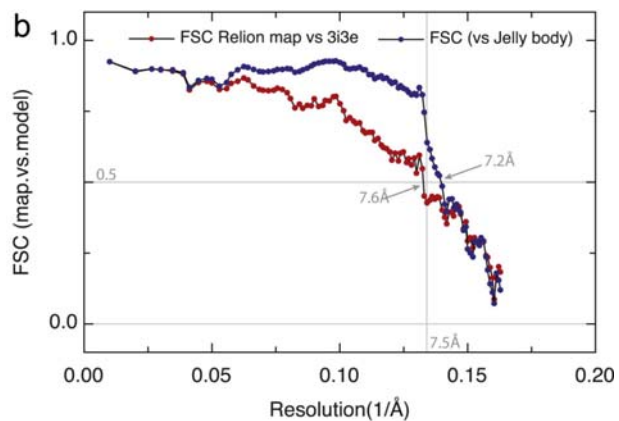
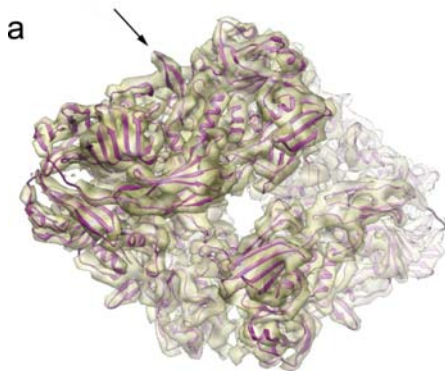
$$FSC_{\text{true}} = (FSC_t - FSC_n) / (1 - FSC_n)$$

(c) The Xmipp package was used with a single reference and weighting to apply low-pass filtering at each cycle. (d) Results of processing the same data using a new program still (McMullan, unpublished) and configured to show substantial overfitting when refined out to 5 Å.

Overfitting is shaded blue, with the difference between the two curves, representing correlations between real features of the structure, shaded pink.

(Chen et al, Ultramicroscopy, 2013)

## Validation of 3D cryoEM maps



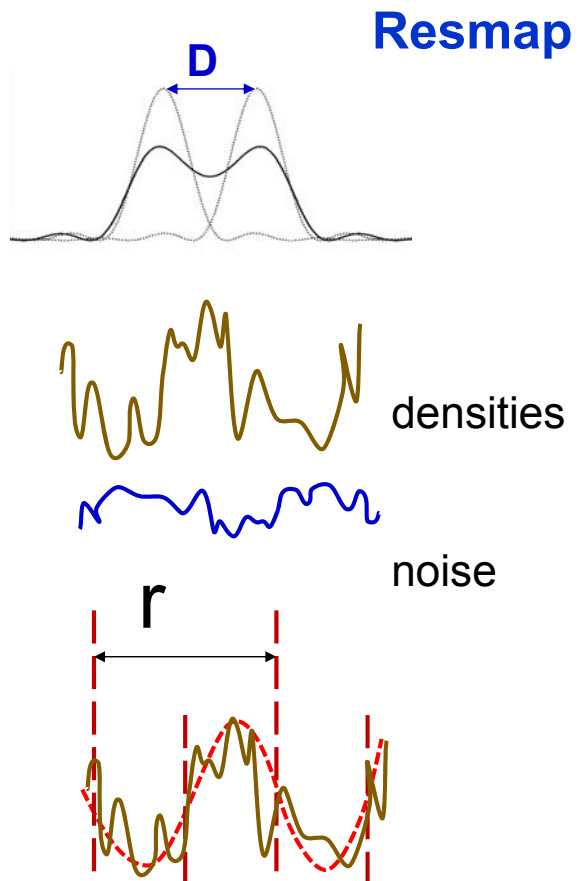
## Resolution estimation

ResMap algorithm is based on initializing a local-sinusoid model at  $r = 2d$ , where  $d$  is the voxel spacing in Å.

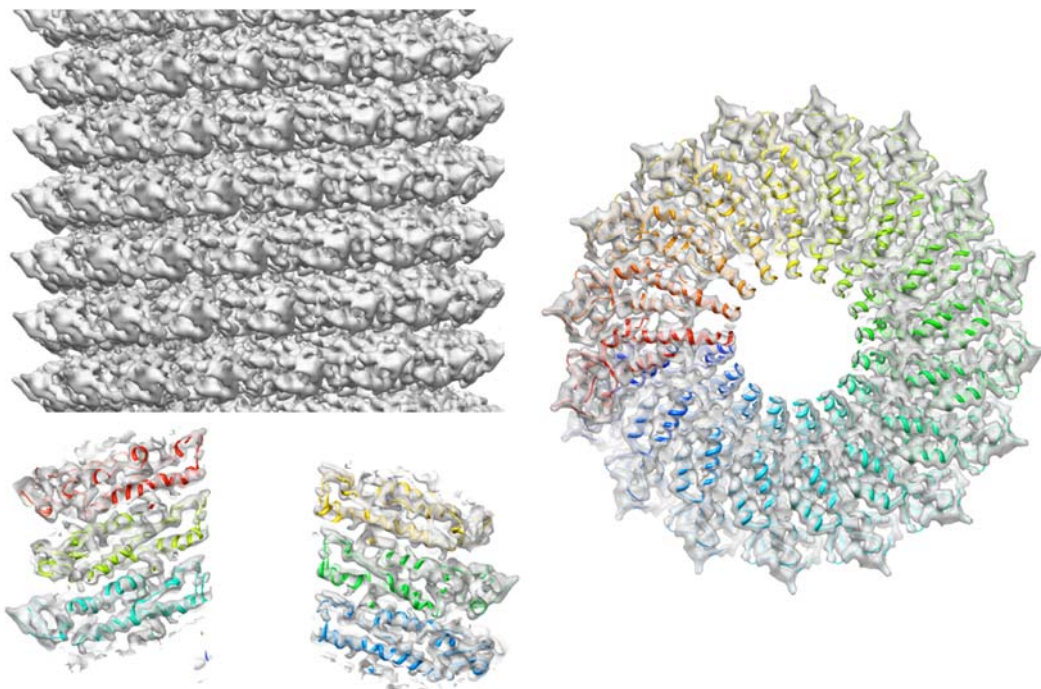
The likelihood-ratio test assess whether a local-sinusoid wave is can describe a local approximation of the model.

The test requires an estimate of the noise variance, which is evaluated from the region surrounding the structure.

The smallest  $r$  gives a local resolution map with a number assigned to every voxel in the density map.



## Tobacco mosaic virus



## Common problems causing defects in reconstruction:

1. The number of projections is small and the pixel size is big
2. The angular range is not uniformly filled
3. Signal/noise ratio is low
4. Projections are not centred
5. Angles are not accurately defined
6. Influence of data acquisition methods (related to #2)
7. In EM the quality of reconstruction results depend on the quality of CTF correction

### Literature:

- Gilbert, P. (1972) **Iterative methods for the three-dimensional reconstruction of an object from projections.**, *J. Theor. Biol.*, 36, 105-117
- Crowther, R.A., DeRosier, D.J., and Klug, A. (1970) **The reconstruction of a three-dimensional structure from projections and its application to electron microscopy.** *Proc. R.Soc. Lond*, 317, 319-340
- Crowther, R.A. (1971) **Procedures for three-dimensional reconstruction of spherical viruses by Fourier synthesis from electron micrographs.** *Philos. Trans. R. Soc. Lond*, B, 261, 221-230
- Radermacher, M. (1988) **Three-dimensional reconstruction of single particles from random and non-random tilt series.** *J. Elect. Microsc. Tech.*, 9, 359-394.
- Harauz, G. and van Heel, M. (1986) **Exact filters for general geometry three dimensional reconstruction.** *Optik*, 73, 146-156
- van Heel, M. and Harauz, G. (1986) **Resolution criteria for three dimensional reconstruction.** *Optik*, 73, 119-122
- Rosenthal PB, Henderson R. (2003) **Optimal determination of particle orientation, absolute hand, and contrast loss in single-particle electron cryomicroscopy.** *J Mol Biol*, 333, 721-45 .
- Saxton, W.O., and Baumeister, W. (1982) **The correlation averaging of regularly arranged bacterial cell envelope protein.** *J. Microsc*, 127, 127-138
- Unser, M., Trus, B.L., and Steven, A.C. (1987) **A new resolution criterion based on spectral signal-to-noise ratios.** *Ultramicroscopy*, 23, 39-52

POCS – projections onto convex sets.

Youla, D.C., and Webb, H. (1982) **Image restoration by the method of convex projections. I. Theory**, *IEEE Trans. Med. Imaging.* 1, 81-94

Sezan, M.I., and Stark, H. (1982) **Image restoration by the method of convex projections. II. Applications and numerical results**. *IEEE Trans. Med. Imaging.* 1, 95-101

Maximum Entropy Method -> Jaynes E.T. (1985) **Where do we go from here? In Maximum Entropy and Bayesian Methods in Inverse Problem** (C.R. Smith, W.T. Grandy Eds) D.Reidel Publishing Co., Dordrecht, Holland, 21-58



## ACKNOWLEDGMENTS



*Athanasios Ignatiou*

*Dan Clare*

*Helen White*

*Helen Saibil*

*David Houldershaw*

*Richard Westlake*

*Benjamin Bammes (DE)*

*Chris Booth (Gatan)*

**welcome**trust

